Self-Consistent Brownian Dynamics Simulation of Polymer Brushes under Shear

Marina G. Saphiannikova,[†] Victor A. Pryamitsyn,[‡] and Terence Cosgrove*

School of Chemistry, University of Bristol, Cantock's Close, Bristol BS8 1TS, U.K.

Received December 11, 1997; Revised Manuscript Received July 6, 1998

ABSTRACT: A novel Brownian dynamics method has been developed to simulate the properties of polymer brushes under shear. Simulations of 100 chains with a chain length of 100 segments have been carried out for a range of shear rates. Compared to previous methods there is a substantial saving in computational time as the self-consistent molecular field method has been chosen to calculate the volume interactions between polymer segments. An important criterion for observing significant deformations of the brush is that the chains must be stretched to beyond the Gaussian threshold. Density profiles and end segment distribution functions for the grafted chains have been determined and show a collapse of the brush under shear in a way similar to that in which a brush contracts in a poor solvent. In particular, the free ends of the chains become concentrated in a narrow region at the periphery of the brush. The number of chains that are affected by shear has also been calculated and shows that there is a progressive transmission of shear into the brush.

Introduction

Rheological studies of interfacial polymer layers are very important for applications such as lubrication and stabilization of thixotropic colloids, adhesion, etc. An important example of an interfacial polymer layer system is an end-grafted dense polymer brush. These systems have been the subject of very intensive theoretical and experimental studies for the last 15 years (see ref 1, for review). Although there has been substantial progress in the understanding of equilibrium properties of such objects, there is no explicit understanding of their nonequilibrium properties. The main results of the equilibrium theory of polymer brushes confirmed by simulation and experiment are that the chains are strongly stretched and the height of the polymer brush h_b is proportional to the length of the polymer chains Na (N is the number of segments, a is the length of the Kuhn segment) and that the free ends of polymer chains are distributed over the entire brush extent (the scale of fluctuations of free ends is of the order of the brush size).

The extent of the brush is determined by a balance between the osmotic pressure of the polymer segments which tends to expand the brush, and the elasticity of polymer chains that opposes it. Shear flow can affect a brush immersed in solvent by the penetration of the solvent flow into the brush, which stretches the polymer chains (Figure 1). In principle, this may change the features of the interaction between polymer segments and the elasticity of the chains. However, the circumstantial evidence given by simulations of polymer brushes under shear[2−7] indicates that interactions between segments in the polymer brush are not affected by the shear, as we discuss below.

When a stretching force, f, applied to the chain does not exceed the "Gaussian threshold" $fa/k_BT \ll 1$(note that this criterion does not depend on chain length) the chains behave as springs with constant elasticity. Here k_B is the Boltzmann constant and T is the absolute temperature. Hence, in this case shear does not change the balance between osmotic pressure and elasticity in the brush, and thus the size and any segmental distribution functions in the brush, averaged in the lateral dimensions, are not affected by the flow. A force stronger than this limit causes the chains to become stiffer,[8] and one can expect a collapse of the brush. In this context, "stiffer" means that the relative elasticity of the polymer chains $\delta x/\delta f$ (here δx denotes the chain extension) decreases with the increasing stretching force f. The equilibrium properties of polymer brushes of non-Gaussian chains were analyzed in ref 8.

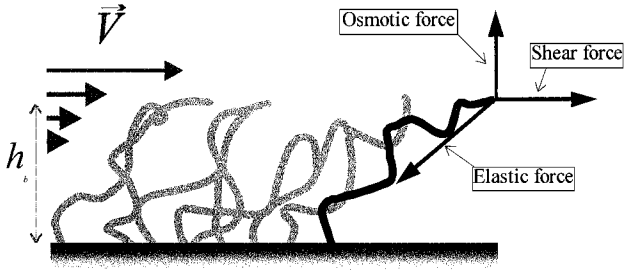

Figure 1. Polymer brush under shear flow: the length of the arrows indicates the solvent velocity.

The problem of penetration of a weak steady shear flow into the polymer brush was analyzed by Milner.[9] In that case the deformations of the polymer chains are linear and the polymer segment density profile of the brush is not affected by the shear (see above). This work utilized the Brinkman equation:[10]

$$\frac{d^2V_x(y)}{dy^2} = \frac{\zeta[\rho(y)]}{\eta}\rho(y)\,V_x(y) + \frac{\nabla p}{\eta} \qquad (1)$$

where $V_x(y)$ is the velocity of the shear flow, $\rho(y)$ is the local density of the polymer brush, ζ is a polymer−solvent friction coefficient, ∇p is the pressure gradient (for pure shear $\nabla p = 0$) and η is the viscosity of the

[†] Institute of Macromolecular Compounds, Russian Academy of Sciences, 31 Bolshoi pr., V. O. 199004 St. Petersburg, Russia.

[‡] Institute of Problems of Mechanical Engineering, Russian Academy of Sciences, 61 Bolshoi pr., V. O. 199178 St. Petersburg, Russia. Present address: Department of Physics and Astronomy, University of Leeds, Leeds LS2 9JT, U.K.

S0024-9297(97)01808-1 CCC: $15.00
Published on Web 09/03/1998

solvent. Here the *x*-axis is parallel to the direction of a shear flow and the *y*-axis is perpendicular to the grafting surface. Milner suggested that $\zeta[\rho] \propto \rho$ and estimated the relative penetration depth $l_p/h_b \propto N^{-1/2}$.[9] Doyle et al. used a friction coefficient, ζ, related to η through Stokes' law $\zeta = 3\pi\eta a$.[4] For this case $l_p/h_b \propto N^{-2/3}$. One can see that the relative penetration of a shear flow is very small for brushes composed of long chains.

If one compares this result with the well-established facts that chains in the brush are stretched and the free ends of the chains are distributed over the brush profile, it is evident that only a small fraction, δ, of the chains in the brush are directly affected by the shear (in the case of weak shear).

Some analytical theories of polymer brushes under shear flow[11−14] are based on the Alexander model.[15] In this "box" model all chains are equally stretched and all the chain ends lie on the outermost point of the brush profile. As a result, all chains are directly affected by the shear. This model is thus not adequate for a polymer brush under shear flow with a distribution in the positions of the chain ends and therefore predictions in these papers[12−14] (for example, the swelling of the polymer brush under shear flow) may be in error.

Unfortunately, it is very difficult to investigate the behavior of dense polymer brushes by computer simulations because these systems are characterized by very long structural relaxation times.[16] Three different methods of computer simulation have been used to investigate polymer brushes under shear: molecular dynamics (MD),[2,3] Brownian dynamics (BD)[4,17] and the dynamic Monte Carlo (MC) technique.[5−7]

Some of the most interesting studies were carried out by Grest.[2,3] These were MD simulations of 50 end-grafted chains of length $N = 100$ immersed in an explicit solvent of dimers. The maximum value of the dimensionless grafting density $\sigma = 0.10$ (number of polymer chains per unit area a^2). He found that the solvent velocity field penetrates only a short distance into the brush, consistent with predictions based on self-consistent field theory[9] and results obtained in an earlier study by Lai and Binder.[5]

It is instructive to calculate the actual shear force in the studies by Grest. The shear force per chain is equal to $f_x = \varpi/\delta\sigma$ where

$$\varpi = \frac{\dot{\gamma}\eta a^3}{k_B T} \tag{2}$$

is the dimensionless shear stress and $\dot{\gamma}$ is the shear rate. (An example: for a polystyrene molecule with $a = 20$ Å at $T = 300$ K the value $\varpi = 1$ corresponds to a shear stress of ∼5 bar). In this way, we estimate that Grest used $\varpi = 10^{-3}$, 5×10^{-3}, and 10^{-2}. One can see that these values do not exceed the Gaussian threshold. For the maximum shear, $f_x \approx 0.1/\delta$. We cannot estimate δ from Grest's data, but in our simulation (see below) δ is varied from $\delta \cong 0.02$ for $\varpi \ll 1$ to $\delta \cong 0.13$ for $\varpi = 1.0$. This means that only for the highest shear rate in the study by Grest were some chains stretched beyond the Gaussian threshold. It is not surprising therefore that only a slight decrease of the brush height was found for the shear rates used by Grest.[2,3]

Doyle et al. studied the behavior of polymer brushes under steady and oscillatory shear by BD simulation.[4] The velocity field was solved self-consistently using the Brinkman equation. The brush was composed of 20 chains of 20 beads each and grafting density of $\sigma = 0.125$. The values of ϖ employed were essentially larger than those investigated in all another simulations: ϖ varied from 0.001 to 1.0. It was found that the brush height remains at its equilibrium plateau value until $\varpi = 0.02$, after which the layer dramatically thins. The flow makes the brush more compact. In his review, Grest[3] accounted for the large decrease in the brush height observed by Doyle et al.[4] to the fact that their chains were extremely short. However, as one can see, the large effect is caused by the large values of the effective shear rate (the Gaussian threshold is *N*-independent).

The first MC simulations were carried out by Lai and Binder.[5] In their study the brush was exposed to a shear flow modeled by a nonequilibrium MC method where the jump rate of effective monomers to neighboring lattice sites in the direction against the flow is smaller than in the flow direction. This assumes that the difference in jump rates is proportional to the local velocity of the flowing fluid. The screening of the velocity field was approximated by the Brinkman equation using a parabolic density profile for the brush whose height was determined self-consistently. It was found that the layer thickness decreased very slightly when solvent flow passed through the brush. The maximum value of N was 60, and the maximum value of σ was 0.0625 for this particular system composed of 64 chains. Lai and Lai continued this study by employing larger values of shear rate.[6]

In more sophisticated MC simulations performed by Miao et al.[7] the velocity profile was also determined self-consistently using the Brinkman equation. However, the authors did not assume a parabolic density profile (as did Lai and Binder[5]). The chain length chosen was $N = 100$, and the grafting density was $\sigma = 0.10$ (using 100 chains). Their simulation results are entirely consistent with those obtained by Lai and Binder.[5] Miao et al. found that the significant response of the brush to the shear flow consisted principally of the axis of the chain tilting toward and stretching of the chain along the direction of the flow, whereas the height of the brush remained essentially unaffected by the flow.

We are unable to estimate values of ϖ for the calculations of Lai and Binder,[5] Lai and Lai,[6] and Miao et al.[7] The snapshots of polymer chain conformations of refs 5 and 7 indicate that the shear was less than that in Grest's simulations.[2,3] Furthermore, these authors used an algorithm for calculating the shear force that was not entirely self-consistent. That is, they calculated the velocity profile using the Brinkman equation with $\zeta[\rho] \propto \rho^{1/2}$; however the friction coefficient used for calculating the stretching force applied to a polymer chain was concentration independent. This means that for this model the force applied by the polymer brush to the flow was not equal to the force applied by the flow to the polymer brush (which is therefore inconsistent with Newton's third law).

The most important result, which can be extracted from these simulations, is that the structure of the brush in the normal direction is not affected by shear until the Gaussian threshold is reached. This means that the system keeps a balance between the elasticity of the polymer chains and the osmotic pressure of the polymer segments. But the elasticity of the chains is constant in this region. This suggests to us that the

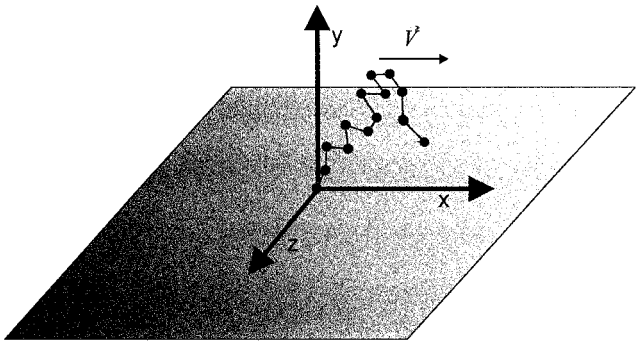

Figure 2. Freely jointed chain near the surface.

volume interactions in the brush do not "feel" the elastic deformations caused by the shear.

Self-Consistent Brownian Dynamics Method

Brownian dynamics simulations have been used to study the polymer brush under the influence of a shear flow. In this method, the atomistic description of molecular dynamics when polymer molecules interact with solvent molecules and other polymer molecules is reduced to a description where polymer molecules interact solely with a continuous viscous media with stochastic time fluctuations.

Doyle et al. utilized a BD algorithm that included explicit calculations of volume interactions between polymer segments and a self-consistent procedure for the calculation of the average shear flow. This was calculated from the average density profile given by the Brinkman equation (eq 1) with a friction coefficient, ζ, related to the solvent viscosity, η, through Stokes' law $\zeta = 3\pi\eta a$.[4] However, if one chooses a self-consistent procedure to calculate hydrodynamic interactions in the system, it is not necessary to use an explicit calculation of the volume interactions. It is well-known that the overall accuracy of an approximation is determined by the strongest approximation being applied. Hence, we chose a self-consistent molecular field method to calculate the volume interactions between polymer segments, which enables the simulation of large systems.

The brush is represented by an assembly of noninteracting polymer molecules, end grafted to an impenetrable surface whose structure is determined by the self-consistent molecular field, and the self-consistent shear flow. The presence of the grafting surface is accounted for by a direct prohibition of moves of the segments below the surface.

Chain model. A freely jointed chain is chosen as a model for the polymer molecule (Figure 2). The number of beads, N, is equal to 101. The first bead is placed at the origin of the Cartesian coordinate system with the y-axis perpendicular to the grafting surface and the x-axis parallel to the direction of the shear flow.

Algorithm. A Brownian dynamics algorithm is used that is governed by a system of Langevin equations to describe the motions of chain beads:

$$\vec{F}^{(l)}_{\text{react}} + \vec{F}^{(l)}_{\text{b}} + \vec{F}^{(l)}_{\text{h}} + \nabla\vec{U}_{\text{mf}}(\vec{r}_l) = 0, \qquad l = 1, 2, ..., N \tag{3}$$

The tensions in the segments, $\vec{F}^{(l)}_{\text{react}}$, which serve to conserve the segment length a, are given by

$$\vec{F}^{(l)}_{\text{react}} = -\frac{\partial U(\vec{b}_l)}{\partial \vec{r}_l} - \frac{\partial U(\vec{b}_{l+1})}{\partial \vec{r}_l} \qquad U(\vec{b}_l) = K\left(\vec{b}_l^{\,2} + \frac{1}{\vec{b}_l^{\,2}}\right) \tag{4}$$

where $\vec{b}_l = \vec{r}_l - \vec{r}_{l-l}$ is a bond vector and $\vec{r}_l$, is the position vector of chain bead l. The value of the elastic coefficient K was chosen large enough ($K = 80k_BT$) to provide a fixed bond length until very high stretching.

$\vec{F}^{(l)}_{\text{b}}$ represents the random Brownian force to which bead l is subjected. The distribution of random Brownian forces is Gaussian and is completely characterized by the first two moments $\langle\vec{F}^{(l)}_{\text{b}}\rangle$ and $\langle(\vec{F}^{(l)}_{\text{b}})^2\rangle$. For polymer models, with a constant friction coefficient of segments, the mean value of the Brownian force $\langle\vec{F}^{(l)}_{\text{b}}\rangle = 0$ and $\langle(\vec{F}^{(l)}_{\text{b}})^2\rangle = (6k_BT/\zeta)\Delta t$.[18]

The hydrodynamic force is described as

$$\vec{F}^{(l)}_{\text{h}} = \zeta\left\{\vec{V}(\vec{r}_l(t)) - \frac{\partial\vec{r}_l(t)}{\partial t}\right\} \tag{5}$$

where $\vec{V}(\vec{r}_l(t))$ is the average local flow velocity. In our case of pure shear flow, it is equal to $V_x(y(t))$, and $\partial\vec{r}_l(t)/\partial t$ is the velocity of bead l at time t. The last term in the Langevin equations represents the gradient of the potential molecular field, which will be described in detail in the following section.

The Langevin equations can be rewritten in finite difference form as follows:

$$\vec{r}_l(t + \Delta t) = \vec{r}_l(t) + \frac{\Delta t}{\zeta}\{\zeta\vec{V}(\vec{r}_l(t)) + \vec{F}^{(l)}_{\text{react}} + \vec{F}^{(l)}_{\text{b}} + \nabla\vec{U}_{\text{mf}}(\vec{r}_l)\} \tag{6}$$

In this form the equations were solved numerically. The segment length a, energy k_BT, and bead friction coefficient ζ are chosen as basis units so that the unit of time is $\lambda = \zeta a^2/k_BT$. The second-order trapezoidal method with one iteration and a time step $\Delta t = 0.0005\lambda$ was used for the integration.

Accumulation of the Density Profile. The most obvious method to accumulate the brush density profile under shear is to obtain the trajectory of one chain in an external field. However, in this case the time needed to obtain adequate statistics for a reliable density profile is extremely large. This is due to the so-called "critical retardation" of the free end fluctuations of a polymer molecule inside the monodisperse brush, where the free end relaxation time $\tau \propto N^3$.[16]

To reduce computer time, we exploit the fact that the time scale of the density profile relaxation appears to be much less than that of a single chain in a monodisperse brush. The long-scale relaxation modes of a particular chain are not of interest here. Moreover, this retardation behavior is specific only for monodisperse systems and is not manifested in polydisperse ones.

We choose a representative assembly of noninteracting molecules, which all have different initial conformations and are all affected by different stochastic forces but are placed in the same external field. The resulting density profile that determines the molecular field for the next iteration can be accumulated during local time scales that are independent of N. Note that this approach is similar to the BD algorithm used by Doyle et al.[4] The main difference is that in our self-consistent

procedure there are no explicit volume interactions between the chains.

Molecular Field. The local exchange chemical potential of the polymer chains is $\mu(y) = \partial f_{int}(y)/\partial\rho$, where $f_{int}(y)$ is the local density of the free energy of volume interactions in the Flory−Huggins approximation, $f_{int} = a^{-3}(1 - a^3\rho)\log[1 - a^3\rho]$ and is used as the potential of the molecular field similar to Scheutjens−Fleer self-consistent field theory:[19]

$$U_{mf}(y) = \mu(y) = -\ln(1 - \rho(y)\cdot a^3) \qquad (7)$$

A cubic spline interpolation of the density profile $\rho(y)$ is used to calculate the molecular field force $\nabla U_{mf}[\rho(y)]$ at every space point.

Shear Flow. The shear flow is calculated by using eq 1 with $\nabla p = 0$ and the friction coefficient, ζ, is related to η through Stokes' law $\zeta = 3\pi\eta a$. The boundary conditions are

$$V_x|_{y=0} = 0 \qquad \frac{\eta a^3}{kT}\frac{dV_x}{dy}\bigg|_{\rho=0} = \varpi$$

Self-Consistent Procedure. The self-consistent procedure can be described by the following symbolic equation:

$$\rho(y) = \overline{BD}\{U_{mf}[\rho(y)],\ V_x[\rho(y)]\} \qquad (8)$$

where $\overline{BD}$ is a symbolic name of the BD procedure that accumulates the density profile of the assembly of noninteracting polymer chains in the molecular field. $U_{mf}[\rho(y)]$ is calculated from eq 7, and the solvent shear flow $V_x[\rho(y)]$ is calculated from eq 1.

One can solve eq 8 numerically by a simple iteration algorithm. To provide stable convergence, it is necessary to increase the number of chains in the assembly, M, and decrease the number of time steps per one iteration n_t. For M, the limitation is simply the computer resources, whereas for n_t, it is the necessity to obtain representative statistics for the density profile accumulated during one iteration step. In principle, such a technique does not require any regularization and can be used to study kinetic processes in polymer brushes. However, the required computer time may still be very high.

Another useful regularization of the simple iteration algorithm is to use the regularized density ρ^*:

$$\rho_i^*(y) = \rho_i(y)\cdot\epsilon + \rho_{i-1}^*(y)\cdot(1 - \epsilon), \qquad 0 < \epsilon < 1 \quad (9)$$

in subsequent iterations. This suppresses oscillations of the density profile between subsequent iterations and leads to a stabilization of the self-consistent algorithm without increasing M.

We have introduced an assembly consisting of $M = 100$ chains and written a parallel code to run it on a SGI Power Challenge multiprocessor system. As we performed our simulations on a machine with four processors, four independent random-number sequences were generated such that each one corresponds to a group of 25 chains. The number of time steps per one iteration, n_t, was equal to 100. For our particular system we used $\epsilon = 0.1$, which suppresses small oscillations of the density profile in the region of chain tails and improves convergence of the self-consistent algorithm on the shear flow.

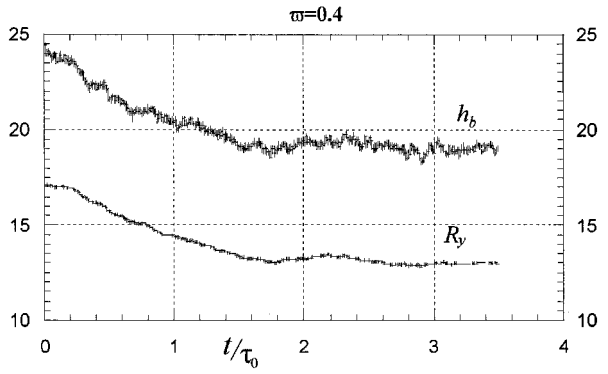

Figure 3. Dependencies of mean-square height of the segments $R_y(t)$ and mean-square height of the brush $h_b(t)$ during the process of establishing of stationary state of the brush. $\tau_0 = \lambda N^2/24$ is the Rouse's relaxation time of the polymer chain.

We performed simulations for the following values of the dimensionless shear rates: $\varpi = 0.001$, 0.1, 0.2, 0.4, 0.6, 0.8, 1.0. The run for a particular shear rate was started using initial chain conformations obtained from a neighboring shear rate. During the simulation procedure, the gradual establishment of a stationary state characteristic of a given value of the shear rate is observed. It takes about 10 000 iterations to attain the stationary state, and the same number of iterations is used to accumulate average distribution functions.

Calculated Distributions and Values. The overall brush density profile, $\rho(y)$, and the distribution of the free end of a polymer chain, $g(y)$, in the direction perpendicular to the grafting surface were obtained. The density profile is normalized by taking into account the value of the grafting density. All simulations where performed for $\sigma = 0.10$.

The process of establishing a stationary state is controlled by tracing the run-time dependencies:

$$R_y^2(t) = \frac{\int_0^\infty y^2\,\rho(y)\,dy}{(N-1)\sigma} \qquad (10)$$

$$h_b^2(t) = \int_0^\infty y^2\,g(y)\,dy \qquad (11)$$

where $R_y(t)$ is the mean-square height of the segments and $h_b(t)$ is the mean-square height of the free ends of chains in the brush.

Figure 3 shows an example of the process of establishing a stationary state after starting the flow with shear stress $\varpi = 0.4$. One can see that after some time, collapse of the brush occurs and a stationary state is established.

Figures 4 and 5 show the influence of the shear flow on the density profile of the brush, and the free end distribution of the brush. One can see that in the process of collapse of the brush under shear, the polymer density profiles and distributions of free ends change in the same manner as observed during compression of the brush or in the collapse of the brush in a poor solvent.[20] The density profiles change from parabolic to steplike, the free end distributions become sharper; i.e., the chain ends approach the extremes of the brush profile. One finds a good agreement of these profiles and the profiles obtained in refs 2−4, where the explicit volume interactions were taken into account, at the

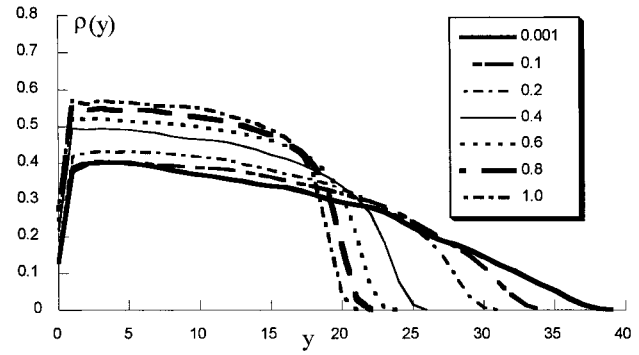

Figure 4. Set of density profiles of the brush at different ϖ.

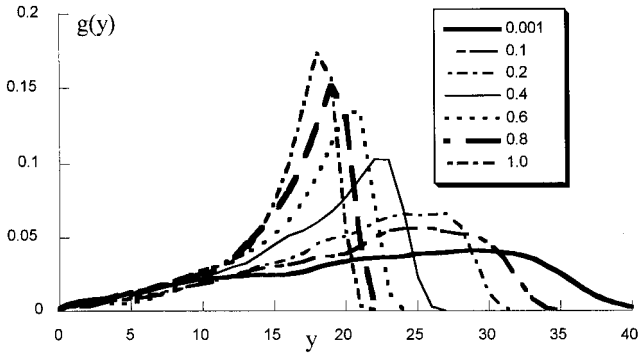

Figure 5. Set of free end distributions in the brush at different ϖ.

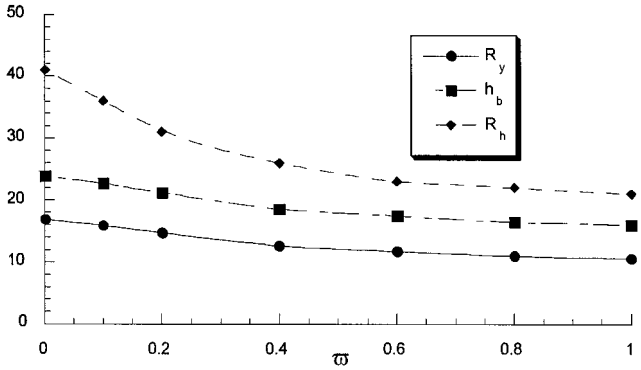

Figure 6. Dependencies of R_y, h_b, and R_h of the brush vs shear stress ϖ.

same values of ϖ ($\varpi = 0.1$ corresponds the maximal ϖ in refs 2 and 3; $\varpi = 1.0$ corresponds the maximal ϖ in ref 4). This means that the self-consistent field approximation is quite adequate to describe volume interactions in polymer brushes under shear.

The dependencies of R_y, h_b, and hydrodynamic height, R_h, of the brush vs shear stress ϖ are shown in Figure 6. We define R_h as the maximum value of y where $\rho(y)$ first becomes equal to 0. The hydrodynamic height decreases more quickly than R_y and h_b by qualitative changes in the density profile from parabolic for smaller ϖ, to steplike at high ϖ. The chain ends are affected much more by the shear, hence the extended profile collapses.

To describe the penetration of the flow into the brush, we introduce a normalized positive function. This function is equal to zero if the polymer density or velocity of shear flow is equal to zero and reaches a maximum in the zone of maximum interaction between flow and the brush. We call this function the "velocity−density overlap function" $\xi(y)$:

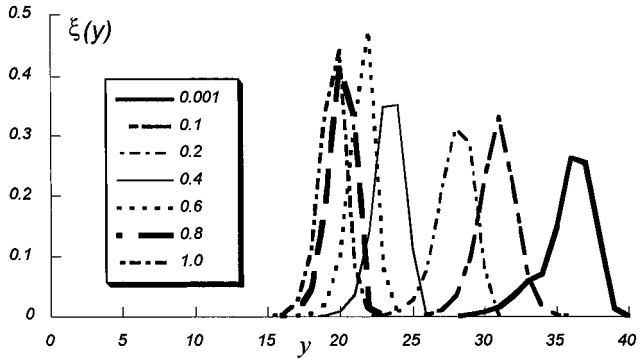

Figure 7. Set of "velocity−density overlap functions" $\xi(y)$ at different ϖ.

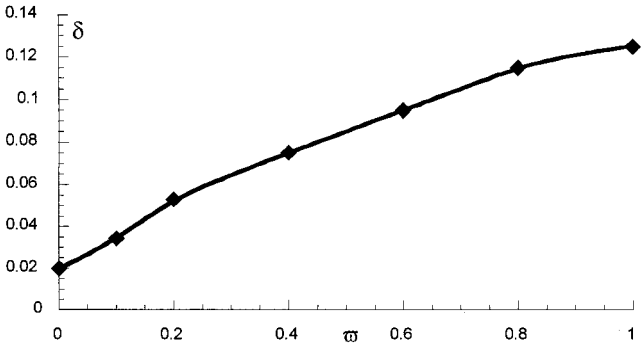

Figure 8. Fraction of the chains directly affected by the shear flow *vs* dimensionless shear stress ϖ.

$$\xi(y) = \frac{\rho(y)\ V_x(y)}{\int_0^\infty \rho(y)\ V_x(y)\ \mathrm{d}y} \tag{12}$$

One can see from Figure 7 that the depth of the penetration of the flow into the brush decreases with increasing shear stress. This is due to the increasing density at the edge of the brush (see Figure 4).

To estimate the fraction of the chains, directly affected by the shear flow, we use a convolution $\delta(\varpi)$ of two positive normalized functions: the "velocity−density overlap function" $\xi(y)$ and the free ends distribution function $g(y)$:

$$\delta(\varpi) = \frac{\int_0^\infty g(y)\ \rho(y)\ V_x(y)\ \mathrm{d}y}{\int_0^\infty \rho(y)\ V_x(y)\ \mathrm{d}y} \tag{13}$$

Figure 8 shows that the fraction of chains, directly affected by the shear flow, δ, increases with shear stress, ϖ, although the depth of penetration of the flow decreases. The reason is the increasing fraction of chains with free ends located near the edge of the brush when it is compressed (see Figure 5). This particular dependence is very "model dependent". If one will use a different dependence of the friction coefficient on polymer density, it will change the dependence $\delta(\varpi)$ qualitatively.

"Average conformations". One of the main aims of the present simulation is to study the inner brush structure. As was mentioned above, the free ends of the chains in the polymer brush are distributed throughout the brush. But if one fixes the free end of a polymer chain in a specific layer in the brush, the fluctuations of the other segments are minimized.[1] In other words, the only fluctuations in the equilibrium brush are the

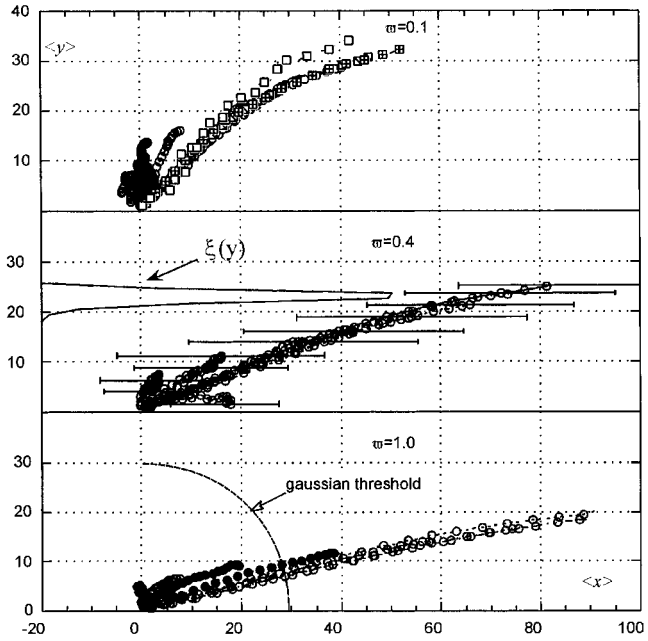

Figure 9. The set of "average conformations" at $\varpi = 0.1$, 0.4, and 1.0. The horizontal bars in the picture $\varpi = 0.4$ show the transverse fluctuations in the free ends positions $\delta\langle x_N^2\rangle$, and the dependence $\xi(y)$ shows the depth of penetration of the flow into the brush. The dashed arc in the plot $\varpi = 1.0$ shows the Gaussian threshold for the stretching of the polymer chains. It corresponds to the size of a freely jointed chain stretched by the force $f = k_BT/a$. (Criterion $fa/k_BT \ll 1$ means that the chain should not be stretched more than one-third of its contour length.

free end fluctuations. So average conformations of chains with their free ends situated in different layers inside the brush may be very informative.

To study this, the space near the grafting surface is divided into layers parallel to the surface. The width of each layer is equal to $2.5a$. The conditional distribution functions $T_x(x,l,m)$ and $T_y(y,l,m)$ have been calculated. They describe the probabilities that the lth bead has the coordinates x or y when the free end of a chain is found in the mth layer. The average trajectories represent the sequences of points, $(\langle x_l\rangle, \langle y_l\rangle)$, $l = 0, 1, ..., N$ with $\langle y_N\rangle \in [2.5ma, 2.5(m + 1)a]$, $m = 0, 1, ..., 19$. Also, we estimate transverse fluctuations in a bead's position $\delta\langle x_l^2\rangle = \langle x_l^3\rangle - \langle x_l\rangle^2$ for every average trajectory.

We have calculated average conformations for all values $\varpi = 0.001$, 0.1, 0.2, 0.4, 0.6, 0.8, 1.0. Figure 9 shows the set of average conformations at $\varpi = 0.1$, 0.4, 1.0. Data in the range $0.1 < \varpi < 1.0$ are qualitatively similar except in the degree of inclination.

One might expect that the average conformations of chains with their ends directly affected by the flow should be inclined, and ones with their ends situated below should be vertical. Figure 9 shows a very unusual effect. Average conformations situated below the zone of direct influence of the flow are also inclined, and the fluctuations of the horizontal positions of the free ends are much larger than the Gaussian size of the polymer coil (for $N = 100$ $\langle R_g\rangle = 10$).

The strong fluctuations of the free ends of the chains may by described as "diffusion flows" of the free ends of the chains up and down the direction normal to the surface. These two "flows" completely compensate each other, giving a stationary density profile of the brush. Also, as was mentioned above, the height of the brush

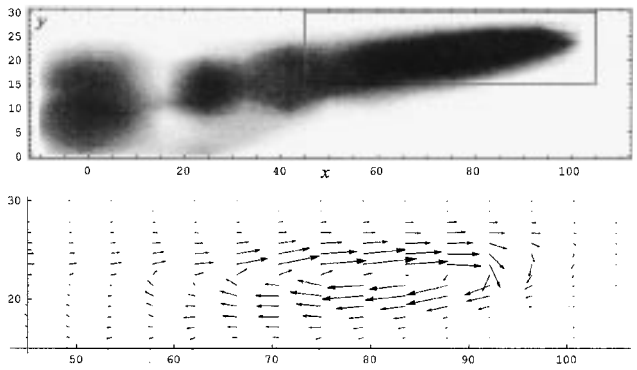

Figure 10. Density plot of the free end distribution function $g(x,y)$ (upper diagram) and a rotational flow of the free ends (lower diagram). The rectangle on the upper diagram corresponds to the range of the lower one. The length of the arrows on the lower diagram corresponds to the average value $\langle \vec{v}_{fe}(x, y)\cdot g(x, y)\rangle$, where $\vec{v}_{fe}$ is the velocity of the chain free end diffusion. Chain is grafted at the point $(x,y) = 0$; $\varpi = 0.4$.

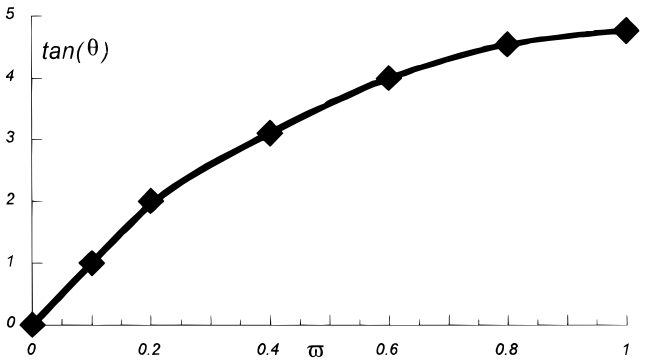

Figure 11. The average slope of the most stretched "averaged conformations" vs ϖ; $\theta = 0$ corresponds to vertical axis.

is defined by the balance between osmotic pressure of the polymer segments and the chain elasticity.

After the end of a chain has penetrated the flow zone, the chain starts to be stretched by the shear flow. When the stretching exceeds the Gaussian threshold, the chain is stiffened. This changes the balance between elasticity and osmotic pressure and the chain contracts toward the surface. Since the stretching is now reduced, the stress is continuously relaxed and the chain becomes less stiff. Finally, the osmotic pressure will force the chain away from the surface. This process can be recognized as the diffusive transfer of shear stress into the zone, which is not directly affected by shear.

To illustrate the appearance of a diffusion flow in the brush, we have drawn a picture of the 2-dimensional free-end distribution function $g(x,y)$, and the free-end flow (Figure 10). This process is nonlinear in nature and is a consequence of the interdependence of the chain extension on its elasticity. Figure 11 shows the dependence of the average inclination of a chain from vertical for the chains in the polymer brush due to shear stress.

Discussion

We have studied the behavior of polymer brushes in strong shear flows. One should be careful in using the term "strong flow" because in this case the value of the shear rate $\dot{\gamma}$ itself does not determine the "strength" of flow.

A dense polymer brush causes significant modification of the imposed flow, which then only penetrates into the upper layer of the brush. We have used the Gaussian

threshold criterion to estimate the actual flow strength for two previous computer simulation studies by Grest[2,3] and Doyle et al.[4] The crossover between weak and strong flows employed in these studies occurs when the value of dimensionless shear stress ϖ is greater than 0.01 and does not depend on the length of the polymer chains.

In the present study a self-consistent Brownian dynamics method was developed, which has allowed us to reduce significantly the CPU time required compared with the CPU time consumed, for example, in the MD study by Grest, where an explicit description of solvent and volume interactions was used. We simplified the atomistic description of the brush structure with a self-consistent molecular field and a self-consistent shear flow. Despite these simplifications, our simulation results are consistent with those obtained by Grest[2,3] and Doyle et al.[4]

Some analytical theories[11−14] describing the behavior of a polymer brush under shear are based on the Alexander model;[15] where all chain ends lie at the extreme end of the brush profile. This "box" model also assumes that one can ignore details of the inner brush structure and consider only the average characteristics of the brush. However, the present simulation shows that despite the tendency of the free ends to approach the extreme of the brush profile under shear, the inner brush structure still differs considerably from the "box" picture. Perhaps this contradiction between the assumptions made in the Alexander theory and the results of more realistic simulations[2−4] explains why the "box" theory prediction of a swelling of the polymer brush under shear is not confirmed by the simulations.[2−4]

As was discussed above, we have found that the depth of flow penetration into the brush does not correlate well with previous work, but we have also found a diffusive penetration of the shear stress into the brush below the flow penetration level. We propose that the static equilibrium of the brush is breaking down under strong shear and some kind of a "dissipative structure" is formed. This process has a nonlinear nature and is caused by the interdependence of the chain extension on its elasticity.

It is known that in polydisperse mixtures of chains, the free ends of each species are confined to distinct layers of the brush and that slow vertical diffusion of the free ends of the polymer chains is suppressed.[16] This means that the transmission of shear diffusion in a polydisperse brush also will be suppressed. We plan to investigate the behavior of polydisperse polymer brushes under shear flow.

Conclusions

The collapse of polymer brushes under shear flow is observed when the "Gaussian threshold" is reached. Under these conditions the brush height strongly decreases, the density profiles become steplike functions and the distribution of free ends of the polymer chains changes its form dramatically. That is, the free ends approach the extremes of the brush profile. Self-consistent shear flow penetrates only into the upper layer of the polymer brush, and this agrees with results obtained previously by Grest.[2,3]

Polymer chains with free ends in the inner layers of the brush are not directly affected by the flow. However, some of them are strongly stretched in the flow direction. This may be explained by the diffusion of the free chain ends in the direction normal to the grafting surface, which causes a diffusion of the shear stress.

However, the resulting picture of the inner structure of a brush under shear does not support a number of hypotheses upon which some existing analytical models are based.

Acknowledgment. We acknowledge support from both NATO and The Royal Society. This work was also partly supported by RFBR (grants 96-03-33862, 96-15-97401), INTAS (grant 93-3372ext), and the Dutch Science Foundation (NWO) grant 047.01.005.96.

References and Notes

(1) Milner, S. T. *Science* **1991**, *251*, 905.
(2) Grest, G. S. In *Dynamics in Small Confined Systems III*: Drake, J. M., Klafter, J., Kopelman, R., Eds.; Materials Research Society: Pittsburgh, 1997; Vol. 464.
(3) Grest, G. S. *Adv. Polym. Sci.*, to be published.
(4) Doyle, P. S.; Shaqfeh, E. S. G.; Gast, A. P. *Phys. Rev. Lett.* **1997**, *78*, 1182.
(5) Lai, P.-Y.; Binder, K. *J. Chem. Phys.* **1993**, *98*, 2366.
(6) Lai, P.-Y.; Lai, C. Y. *Phys. Rev. E* **1996**, *54*, 6958.
(7) Miao, H.; Guo, H.; Zuckermann, M. J. *Macromolecules* **1996**, *29*, 2289.
(8) Amoskov, V. M.; Pryamitsyn, V. A. *J. Chem. Soc., Faraday Trans.* **1994**, *90*, 889.
(9) Milner, S. T. *Macromolecules* **1991**, *24*, 3704.
(10) Brinkman, H. C. *Appl. Sci.* **1947**, *A1*, 27 L.
(11) Rabin, Y.; Alexander, S. *Europhys. Lett.* **1990**, *13*, 49.
(12) Barrat, J.-L. *Macromolecules* **1992**, *25*, 832.
(13) Birshtein, T. M.; Zhulina, E. B. *Makromol. Chem., Theory Simul.* **1992**, *1*, 193.
(14) Harden, J. L.; Cates, M. E. *Phys. Rev. E* **1996**, *53*, 3782.
(15) Alexander, S. *J. Phys. (Paris)* **1977**, *38*, 983.
(16) Klushin, L. I.; Skvortsov, A. M. *Macromolecules* **1992**, *25*, 3443.
(17) Neelov, I. M.; Borisov, O. V.; Binder, K. *Macromol. Theory Simul.* **1998**, *7*, 141.
(18) Fixman, M. *Macromolecules* **1986**, *19*, 1195.
(19) Scheutjens, J. M. H. M.; Fleer, G. J. *J. Phys. Chem.* **1979**, *83*, 1619.
(20) Zhulina, E. B.; Borisov, O. V.; Pryamitsyn, V. A.; Birshtein, T. M. *Macromolecules* **1991**, *24*, 140.

MA971808F